Health-Aware Charging of Li-Ion Batteries Using MPC and Bayesian Degradation Models

Taranjitsingh Singh^{©a}, Jeroen Willems^{©b}, Bruno Depraetere^{©c} and Erik Hostens^{©d}

MotionS, Flanders Make, Lommel, Belgium

fi fl

Keywords: Model Predictive Control (MPC), Health-Aware Charging, Lithium-Ion Batteries, Bayesian Networks.

Abstract:

We propose a Model Predictive Control (MPC) approach for health-aware optimal charging of Lithium-ion Nickel Manganese Cobalt (Li-NMC) batteries. Our method integrates electrical, thermal, and degradation models using Bayesian Networks (BNs) to estimate the battery's State of Health (SOH). These models are embedded into an MPC framework to generate charging profiles that reduce long-term degradation while ensuring fast charging performance. Validation is performed through high-fidelity simulations using the PyBaMM battery modeling environment. Results show improved SOH retention compared to conventional Constant Current-Constant Voltage (CC-CV) strategy.

1 INTRODUCTION

The electric vehicle (EV) market, particularly the part using Lithium-ion Nickel Manganese Cobalt (Li-NMC) batteries, is experiencing significant growth, with forecasts indicating continued expansion in the coming decades. In 2023, nearly 14 million electric cars were sold globally, making up 18% of all EV sales worldwide, indicating a growing trend in sales. This upward trend is expected to continue, with key markets like China, Europe, and the United States at the forefront. As the market expands, the demand for charging infrastructure is also anticipated to rise substantially. To support the increase in electric vehicles, the number of public charging stations will need to grow sixfold by 2035 (Agency, 2024).

Despite advancements, range anxiety and battery aging continue to be significant obstacles to broader EV adoption. Enhancing charging infrastructure is essential, but reducing charging times is equally critical. A smart and fast charging strategy aims to reduce charging time while preserving lithium-ion battery lifespan. This requires precise regulation of charging currents within physical limits to avoid conditions that could cause rapid, unwanted degradation of batteries or, in extreme cases, thermal runaway. Developing

^a https://orcid.org/0000-0003-3255-3796

such a fast charging strategy for EVs with Li-NMC batteries is a complex and resource-intensive task (Wassiliadis et al., 2023).

The standard fast charging protocols used in EVs have long been the classical Constant-Current Constant-Voltage (CC-CV) method (Abdollahi et al., 2016). To mitigate the risk of degradation, these protocols have been extended to include multiple CC phases along with a CV phase (MCC) (Li et al., 2020). Additionally, researchers have explored methods that deliver high C-rate pulses to further preserve battery health (Qin et al., 2022). However, while these methods perform well for slow charging, they are inherently static and fail to provide a charging profile that accounts for the preservation of battery health (Lu et al., 2024).

As previously mentioned, smart fast charging presents the challenge of balancing charging times with battery degradation, which can affect the long-term State-of-Health (SOH) of EV batteries (Agency, 2024). Extensive reviews on fast charging methods, particularly for EVs, have been conducted by researchers, as noted in (Tomaszewska et al., 2019). Their discussions highlight the impact of overcharging on battery degradation. Most fast charging algorithms prioritize avoiding thermal runaways, which leads to a focus on the design part of thermal management rather than the algorithms themselves (Tomaszewska et al., 2019). In the realm of charging algorithm investigations, the research predominantly depends on degradation models, which are empirical-based meth-

^b https://orcid.org/0000-0002-2727-6096

clb https://orcid.org/0000-0003-2011-3857

^d https://orcid.org/0000-0003-2482-7523

ods and so their performance can only be tested for a limited range of chemistries (Tomaszewska et al., 2019; Erdinc et al., 2009).

Despite these difficulties in modeling, incorporating battery degradation into fast charging algorithms is essential. Battery degradation is a complex process resulting from multiple mechanisms within the battery chemistry. Some of the key mechanisms include the formation of a solid electrolyte interphase (SEI) layer on the anode surface, lithium plating — where lithium ions from the electrolyte are deposited as metallic lithium on the anode — and the loss of active materials (Birkl et al., 2017). Fast charging and high currents lead to elevated temperatures, which accelerate these degradation processes, subsequently increasing the anode potential which must be avoided when designing charging profiles.

Advanced health-aware fast charging algorithms exist, where researchers have dived into the use of Model Predictive control (MPC) techniques by including these degradation models in the optimization. One of the first MPC techniques considered for optimal charging dates back to 2011, where the researchers utilized advanced degradation models (Wassiliadis et al., 2023; Klein et al., 2011). Although these models are derived from accurate electrochemical models, they are inherently complex involving multiple states. Consequently, identifying model parameters, or estimating the intermediate states presents a significant computational challenge. Therefore, the studies conducted in (Xavier and Trimboli, 2015; Xavier et al., 2020) employ a reduced-order model of the battery, which is derived from a complex electrochemical model.

In this paper, we use a Bayesian Network (BN) model that relies on the degradation drivers rather than using the electrochemical model states, along with a model for battery and electro-thermal dynamics. This method stands in contrast to the one presented in (Lu et al., 2024) which employs a deterministic parametric state-space model for degradation. The key advantage of our approach is its ability to account for stochastic variations. This method can also be applied in closed-loop simulations to achieve more accurate degradation estimates. Our novelty is in framing the optimal health-aware charging problem as a Nonlinear MPC problem using the BN predicted distributions and conducting realistic high-fidelity simulations for validation.

The article is organized as follows. Section 2 details the proposed models and estimators. Section 3 outlines the formulation of the MPC problem for health-aware charging control. Section 4 presents the validated results, and finally, Section 5 draws the conclusions of this article and provides insights on future research directions.

2 MODELING APPROACH

Figure 1 explains the interconnected modeling framework necessary for health-aware charging optimization. It highlights three necessary models: the Battery Model, the Electro-Thermal Model, and the State of Health Model, which collectively govern the behavior and performance of a battery (Wassiliadis et al., 2023). The Battery Model simulates the relationship between the State of Charge (SOC) and the battery's voltage. The Electro-Thermal Model models the temperature variations, and interactions of temperature with SOC and the SOH. Lastly, the SOH model includes the long-term degradation of the battery, taking into account the operating conditions and impact of various charging strategies.

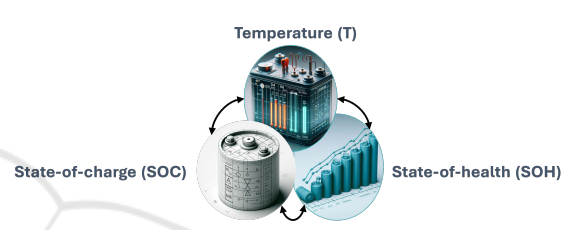


Figure 1: Coupling and interconnected framework required for health-aware charging (Wassiliadis et al., 2023).

This section provides the detailed descriptions of these three models.

2.1 Battery Model

The battery dynamics are modeled using a first-order Resistance-Capacitance (RC) Equivalent Circuit Model (ECM). This describes the relationship between the overpotential o_k and the terminal voltage y_k , as a function of the current u_k . This influence is a function of resistances and capacitances that vary with parameters such as the SOC s_k and temperature T_k . Therefore, the dynamic behavior of T_k and s_k will be modeled as well: for T_k this will be done in the thermal model in the next section, but the evolution of s_k is added here to the ECM model. This yields an overall battery model with states $x_{ECM} = [s_k, o_k]^T$ given by:

$$ECM \left\{ \begin{array}{c} \left[\begin{array}{c} s_{k+1} \\ o_{k+1} \end{array}\right] = \left[\begin{array}{c} 1 & 0 \\ 0 & \theta^1 \end{array}\right] \left[\begin{array}{c} s_k \\ o_k \end{array}\right] + \left[\begin{array}{c} \frac{\Delta t}{Q_k} \\ \frac{\theta^2}{\theta^2} \end{array}\right] u_k \\ y_k = o_k + V^{OCV}(s_k, T_k) + \theta^3 u_k \end{array} \right.$$
(1)

Herein, Q_k expresses the battery's total capacity, $V^{OCV}(s_k, T_k)$ expresses the open-circuit-voltage (OCV) as a function of current, and θ^1 , θ^2 and θ^3 express gains depending on resistances and capacitances that vary over time as a function of s_k and T_k . As a result, this becomes a Linear Parameter Varying – Input Out-

put (LPV-IO) model. We have used experimental logs of voltages, current, temperature, and SOC, to identify these model parameters in multiple conditions using the methodology as given in (Hoekstra et al., 2023).

2.2 Electro-Thermal Model

Now we will describe the thermal behavior of the battery. As seen in the previous section, the parameters of the ECM are influenced by the battery temperature. Likewise, how much the battery heats up, is affected by electrical parameters like the current, the terminal voltage and the OCV. Consequently, there is a mutual coupling and interaction between the ECM and the thermal model (Cai et al., 2021).

The electro-thermal model expresses the heat \dot{q}^{th} generated at the core of the battery, how this affects the core temperature T_c and the surface temperature T_s , as well as how much cooling is obtained at the battery's surface which is in contact with the environment at ambient temperature T_f . This yields the electro-thermal battery models (ETBM) with states $x_{ETBM} = [q_t^{th}, T_{Ct}, T_{St}]^T$ as given by:

$$ETBM \begin{cases} \dot{q}_{k}^{th} = u_{k} \left(V^{OCV}(s_{k}, T_{k}) - y_{k} \right) \\ T_{c_{k+1}} = T_{c_{k}} + \frac{\Delta t}{C_{c}} \left(q_{k}^{th} + \frac{T_{s_{k}} - T_{c_{k}}}{R_{c}} \right) \\ T_{s_{k+1}} = T_{s_{k}} + \frac{\Delta t}{C_{s}} \left(\frac{T_{f_{k}} - T_{s_{k}}}{R_{u}} + \frac{T_{c_{k}} - T_{s_{k}}}{R_{c}} \right) \end{cases}$$
(2)

Here, the first equation expresses the heat generation due to the charging, as the product of the current u, and the voltage which is a function of electrical parameters as mentioned. The second and third equations express the evolution of core and surface temperatures, with C_c and C_s the centralized heat capacity of the battery core and the battery surface respectively. These evolutions are a function of the generated heat and the cooling, as well as of the heat transfer between the two. This transfer is affected by R_c , denoting the equivalent conduction heat resistance used to simulate the heat exchange between the core and the surface, and R_u , denoting the equivalent convective resistance used to simulate the convective cooling on the battery surface.

Remark 1. Note that for simplicity, the temperature T used in the ECM model is taken as the average between T_c and T_s .

2.3 State-of-Health Model

For health-aware control, we need a reliable model for degradation of batteries. Indeed, if we know how degradation evolves as a function of charging and discharging profiles, then (i) it can be included as a cost function for optimal control, and (ii) it can be used to improve the SOH estimation and therefore the SOC estimation, since the latter relies on an accurate knowledge of the actual value of Q_k in (1).

 SOH_k which represents the current state of health, is related to the loss of capacity due to degradation is expressed as follows:

$$SOHM \begin{cases} SOH_{k+1} = \frac{1}{Q_{nom}} (Q_k - \Delta Q_k) \\ \text{or} \end{cases}$$

$$SOH_{k+1} = SOH_k - \frac{\Delta Q_k}{Q_{nom}}$$
(3)

where, Q_k is the current cell's capacity, Q_{nom} in the nominal cell capacity, and ΔQ_k represents the capacity degradation.

While this is a simple model, it is in practice very hard to estimate these quantities correctly. The degradation model therefore needs to include the uncertainty. An accurate quantification of the uncertainty distribution is important as we know that the SOC level has a strong influence on degradation, especially in case of under- and overcharging, for which the tails of the SOC distribution matter. This information is then fused with other sources of information such as sensor inputs (current, voltage, temperatures, etc) or other models such as the SOC to open-circuit voltage relation, to then form a total posterior distribution for the SOC. However, detailed models of degradation, such as (Sulzer et al., 2021) for Li-ion batteries, are too complicated to use in an online optimal control calculation. Furthermore, although these models rely on a profound understanding of the physics of degradation, it is a process that relies on many influences, many of which are unmeasured or even unknown, as such rendering it highly stochastic. This stochastic behavior can be derived from real measurement data only. A useful tool for training stochastic models are Bayesian Networks (BN), as they provide a comprehensible graphical description of all involved variables and their stochastic relations. Especially for SOH and/or remaining useful life (RUL) predictions, where data is censored and models and measurements with their uncertainties have to be fused in a nontrivial way to support maintenance decisions, BNs have proven their usefulness (Hostens et al., 2024).

In this paper, we adopt a simplified use of BNs, and we assume availability of periodic capacity measurements Q in the data. This is motivated by the existence of explicit procedures for capacity measurement, such as (Christophersen, 2015, p14). We then model the change in capacity as a function of the degradation drivers, such as temperature, depth-of-discharge (DoD) and C-rate. Full formulations are provided in Section 4.

In absence of prior knowledge of the nature of these relations, it is recommended to use data-based regression techniques and suggest specific functions and distributions with a low number of parameters. In many cases, generalized linear regression is a good starting point. Training of the BN returns the posterior distribution of the model parameters, as shown in Fig. 2. An ill-chosen model will result in bad convergence, yielding for instance multi-modal posteriors, which can be used to trigger a refinement of the model, or to collect more data (in case of too wide posteriors).

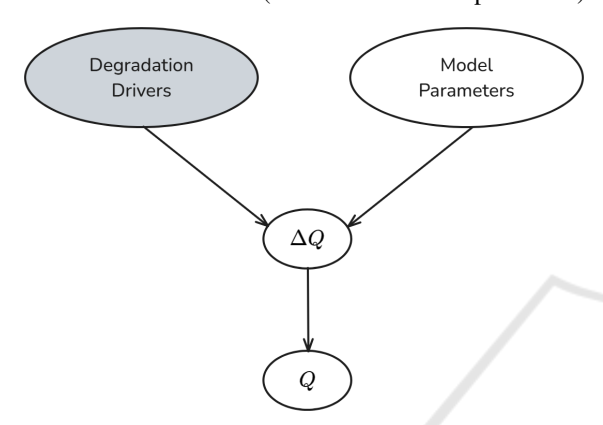


Figure 2: Generic BN representation of battery degradation. The gray-colored variables are observed during training.

3 HEALTH-AWARE PROBLEM FORMULATION

In this section we introduce our problem formulation for the health-aware charging for the lithium ionbatteries.

The trade-off between fast charging and health degradation, is illustrated in Figure 3. It shows the battery's SOC, charging current, and SOH over time, for two different current profiles. The bottom graph illustrates the SOH over time, with the red curve indicating a faster decline in SOH due to aggressive charging, and the blue curve showing less degradation with conservative charging. The overall goal of health-aware charging is to minimize the total charging time, which is to reach the desired SOC as fast as possible, while also minimizing SOH degradation, yielding a trade-off between fast charging and preserving battery health.

Now, to define the Health-aware optimal charging problem formulation, we first gather all needed models. We couple the discretized ECM model (1) with the discretized ETBM model (2) and couple it to the discretized SOH model (3). This results in the collective states, $x = [x_{ECM}, x_{EBTM}, x_{SOH}]$, with $n_x = 6$, and input

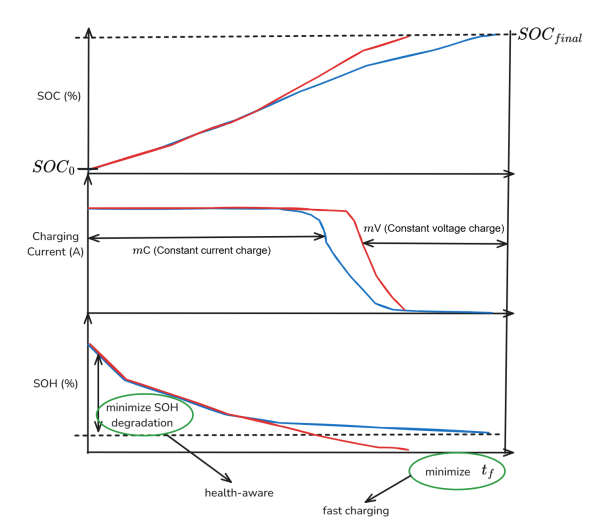


Figure 3: Illustration of the health-aware optimal charging.

u as the current. With that model, the MPC formulation for Health-aware charging can now be formulated as follows.

Formulation 3.1. Given a battery model with the ECM model (1) from section 2.1, the discretized ETBM (2) from section 2.2 and the discretized SOH model mapped from the capacity degradation model from section 2.3, the optimal charging current protocol sequence input sequence $\mathbf{u} = \{u_{0:x_k}, u_{1:x_k}, ..., u_{N_h-1:x_k}\}$ is the one that from an initial SOC, brings the system to the final desired SOC as quickly as possible while preserving SOH:

minimize
$$J(x_k, u_k)$$

subject to
 $J(x_k, u_k)$
 $S_{min} \leq S_k \leq S_{max}$
 $-I_{max} \leq u_k \leq I_{max}$
 $V_{min} \leq y_k \leq V_{max}$
 $T_{min} \leq T_k \leq T_{max}$
 $X_0 = X_0$

(4)

Remark 2. Note: In our MPC formulation, the expected value of the SOH distribution from the Bayesian Network model is used in the optimization cost.

Formulation 3.2. The objective term $\mathcal{J}(x_k, u_k)$ is a sum consisting of the following three terms:

- 1. Fast charging term: $J_1 = Q_s \sum_{k=0}^{N_h} ||s_k s_{final}||_2$. This first objective term penalizes deviations of the SOC from s_{final} , encouraging the SOC to get close to this value.
- 2. Degradation preserving term: $J_2 = Q_{soh} \sum_{k=0}^{N_h} ||SOH_k SOH_0||_2$. This term penalizes

changes in the SOH, promoting preservation in the battery's health.

3. Input regularization: $J_3 = Q_u \sum_{k=0}^{N_h} ||u_{k+1} - u_k||_2^2$. This term penalizes the rate of change of the charging current, promoting smoother current profiles.

The combination of objectives J_1 , J_2 and J_3 ensures a smooth, health-aware charging current \mathbf{u} is obtained, which also ensures the battery is charged sufficiently quickly.

4 VALIDATION RESULTS

4.1 NMC Battery Data Collection

The Oxford Mathematical modeling Battery Group's Python Battery Mathematical Model (PyBaMM) (Sulzer et al., 2021), built on top of CasADi (Andersson et al., 2019), was used to collect efficient battery simulations data. The specific Doyle-Fuller-Newmann (DFN) model for Lithium-ion NMC batteries with electrochemistry as depicted in (O'Kane et al., 2020) for 5Ah was used.

This model is configured with several options that captures various degradation mechanisms and physical phenomena occurring within the battery. For instance, the "SEI" (Solid Electrolyte Interphase) formation is set to be "solvent-diffusion limited", and changes in SEI porosity are enabled. The model also includes options for lithium plating porosity change, particle mechanics (both swelling and cracking), SEI formation on cracks, and stress-driven loss of active material (O'Kane et al., 2022).

The models use a discretization of the different regions of the battery. These regions include the negative electrode (x_n) , separator (x_s) , positive electrode (x_p) , and the particles within the negative (r_n) and positive (r_p) electrodes. The number of regions determines the resolution of the numerical solution in each region, with higher values providing more detailed simulations at the cost of increased computational effort. The used values of the discretization parameters are listed in Table 1.

We performed a series of experiments with several charging protocols and voltage limits. We also included noise to introduce stochasticity in the experiments. A subset of the resulting capacity degradation curves is shown in figure 4.

4.2 Model Parameters

The parameters of the ECM model, i.e., θ^1 , θ^2 , and θ^3 are chosen as polynomial functions. For this spe-

Table 1: Overview of the used discretization parameters for PyBaMM simulations for the cell stoichiometry from (O'Kane et al., 2020).

Parameter Name	Symbol	Value
negative electrode	x_n	5
positive electrode	x_p	5
negative particle	r_n	30
positive particle	r_p	30
separator	x_s	5

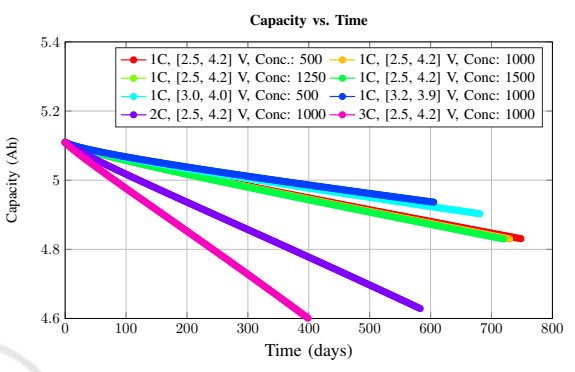


Figure 4: Capacity degradation curves resulting from different degradation mechanisms, with charging protocols varied from 1C-rate, 2C-rate and 3C-rate, along with several values of Depth of Discharge (DoD) and initial concentration in electrolyte [mol.m-3].

cific model, a seventh-order polynomial function of the SOC is selected. The values of their coefficients were estimated from the data using the LPVCore toolbox (den Boef et al., 2021).

Remark 3. On establishing the curves $V^{OCV}(s_k, T_k)$ for the considered cell, it was observed that the sensitivity to temperature was found to be negligible, and so for the results shown in the next subsection, the dependency of T_k was dropped from the V^{OCV} curve, as well as from the polynomial functions θ^1 , θ^2 , and θ^3

The ETBM parameters are extracted from (Akbarzadeh et al., 2020) where they are derived empirically for Lithium-ion NMC battery of 5Ah capacity. The parameters are listed in Table 2:

Table 2: Thermal parameters for ETBM model as extracted from (Akbarzadeh et al., 2020).

Parameter Name	Symbol	Value	Unit
Battery core heat capacity	C_c	934.5	J/kg.K
Battery surface heat capacity	C_s	1661.9	J/kg.K
Conductive heat resistance	R_c	0.422	K/W
Convective cooling resistance	R_u	0.559	K/W
Ambient temperature	T_f	298.18	K

The parameters for the BN degradation models that are used to model the SOHM in (3) for ΔQ , are

trained on simulated accelerated aging data with full charge/discharge cycles. We accordingly modeled the discrete loss of capacity ΔQ after each cycle.

• For charging cycles, ΔQ follows a shifted exponential distribution, or $\Delta Q - \mu_{\rm C} \sim {\rm Exponential}(\lambda_{\rm C})$, where

$$\mu_{C} = \Delta Q_{C,\text{nom}} + \alpha_{C,V} \left(V - V_{C,\text{nom}} \right) + \alpha_{C,I} \left(I - I_{\text{nom}} \right). \tag{5}$$

• For discharging cycles, ΔQ follows a Laplace distribution: $\Delta Q \sim \text{Laplace}(\mu_D, b_D)$, where

$$\mu_{\rm D} = \Delta Q_{\rm D,nom} + \alpha_{D,V} \left(V - V_{\rm D,nom} \right) + \alpha_{D,I} \left(I - I_{\rm nom} \right). \tag{6}$$

The variable V represents the final voltage of the cycle and is as such equivalent to the depth of charge/discharge. The variable I represents the constant current (either during constant load or in CC phase of CC-CV), and is as such equivalent to C-rate. The values for the model parameters and nominal settings are shown in Table 3, and the relative prediction error histograms and corresponding modeled distributions in figure. 5. Note the wide distributions of relative prediction errors, which is due to the intrinsic stochasticity of the degradation process. This emphasizes the importance of correct uncertainty quantification.

Table 3: Model parameter values for degradation models.

parameter	value	unit	parameter	value	unit
$\Delta Q_{\mathrm{C,nom}}$	8.35e-6	Ah	$\Delta Q_{ m D,nom}$	1.21e-5	Ah
$\alpha_{C,V}$	2.47e-5	Ah/V	$\alpha_{D,V}$	-2.83e-5	Ah/V
$\alpha_{C,I}$	2.52e-6	Ah/A	$\alpha_{D,I}$	7.38e-6	Ah/A
$V_{\mathrm{C,nom}}$	3.9	V	$V_{ m D,nom}$	3.25	V
Inom	4	A	$b_{ m D}$	1.93e-6	Ah
$1/\lambda_{\rm C}$	2.71e-6	Ah			

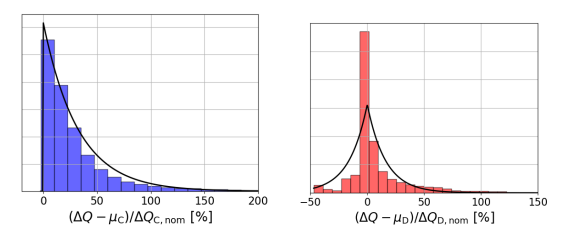


Figure 5: The histograms for the relative prediction errors of ΔQ and corresponding modeled distributions (black), for charging (blue, left) and discharging (red, right).

4.3 Results

The MPC formulation 3.1 is implemented in CasADi (Andersson et al., 2019) and Rockit framework (Gillis et al., 2020) for testing in simulations in Python. To solve the optimization, we used the interior point based IPOPT solver (Wächter and Biegler, 2006) interfaced with CasADi. The simulation was carried

out on a PC with an Intel(R) Core(TM) Ultra 7 155H and 32GB memory.

The parameters selected for the controllers are detailed in Table 4. As can be seen, we calculated our charging profiles using various C-rates, as well as different weights for how much to promote fast charging. This allows us to validate the robustness of our method under different conditions.

Table 4: Overview of MPC formulation parameters for the health-aware charging.

MPC parameters	symbol	value
Symbolic framework	-	CasADi
Solver	-	IPOPT
MPC Horizon	N_h	250 samples
Time for trajectory	T	3600s
C-rates	I_{max}	[1,2,3] C
SOC constraints	$[s_{min}, s_{max}]^T$	$[0.2, 0.8]^T$
SOC charging ref.	Sfinal	0.8 ightarrow 80%
Initial Temperature	Tinit	297 K
Weight (SOH deg.)	Q_{soh}	10^{-3}
Weight (Δu)	Q_u	10^{-2}
Weight (fast charging)	Q_s	$[10^{-4}, 10^{-3}, 10^{-2}, 1, 10]$

The simulations are performed with optimal health-aware charging at different C-rates, aiming to bring SOC from 0.2 to 0.8 (i.e. from 20% to 80%.) This approach follows recommendations suggesting that at low operating SOCs, significant degradation may occur due to rapid volume expansion (Bazlen et al., 2022). Figure 6 shows the simulated results of Current vs SOC achieved with the optimal control at different C-rates and with different weights Q_s . The transparency of the curves decreases as the weight Q_s is increased. It can be seen that the control yields a set of charging profiles, that all bring the SOC to the desired value according to the allowed C-rate, but at different rates depending on the choice of Q_s .

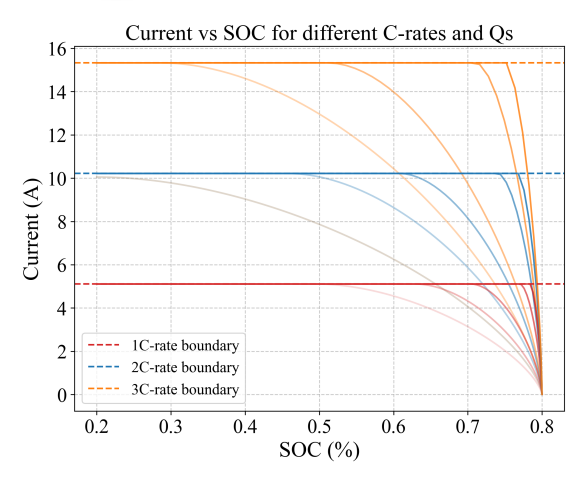


Figure 6: Simulation results for charging currents vs. SOC at 1C, 2C and 3C rates with varying Q_s .

Figure 7 shows the corresponding trajectories of the SOCs, SOHs and Voltage along with optimal charging current as a function of time, for the 3C rate. Again, as Q_s increases, the curves become less opaque. It can be observed that the fastest charging has the highest SOH degradation. Note that in this graph we have shown the 3C rate. This is the one we would use for health-aware but still fast charging, since for fast charging according to "IEC6581-1 EV charging mode 4" the entire battery has to be charged within 15-20 minutes (Van Den Bossche, 2010).

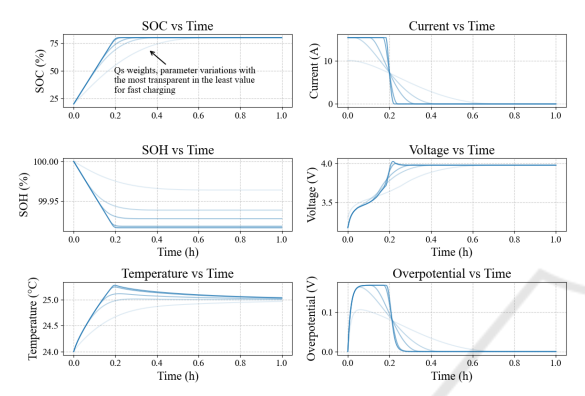


Figure 7: Simulation results of the optimal input and states: SOC, SOH, Voltage, Temperature and Overpotential for 3C fast charging with varying Q_s .

In order to further validate our proposed approach, we compare the health-aware charging protocol to the conventional CC-CV charging strategy. Here we have used both to charge the SOC from 20% to 80%, assuming an initial SOH of 100%. After charging, we then discharged using a 3C discharge profile, like in (Abdollahi et al., 2016). The result of this comparative analysis for a cycle is shown in Figure 8. The SOH degradation for CC-CV charging is determined postprocess, once the charging profile has been established. As illustrated in the figure, the CC-CV method results in noticeably higher degradation. This increased degradation can be attributed to an overshoot in terminal voltage and the absence of an integrated SOH model during the charging process, indicating suboptimal charging.

Next, we simulate a prolonged sequence of charge cycles, where in between the cycles we also estimate the changes in SOH with the BN approach described above. To make this a realistic sequence we use data from the Urban Dynamometer Driving Schedule (UDDS), developed by the Environmental Protection Agency (EPA) that simulates city driving conditions. The UDDS driving cycle is a standardized driving cycle used for vehicle testing (Plett, 2004). From it, we derive the scaled discharge current profiles from the speed profile of UDDS, and then repeat it to generate

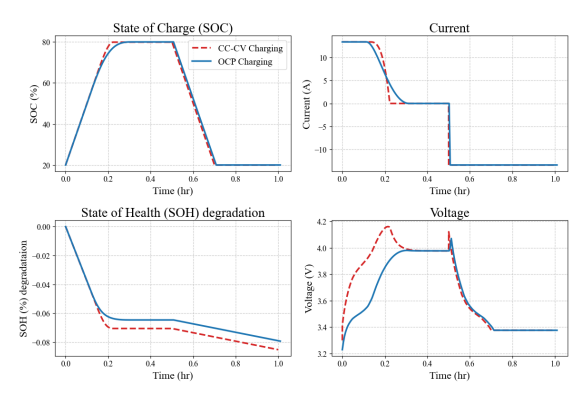


Figure 8: Charge and Discharge cycle comparison of Healthaware optimal charging with standard CC and CV.

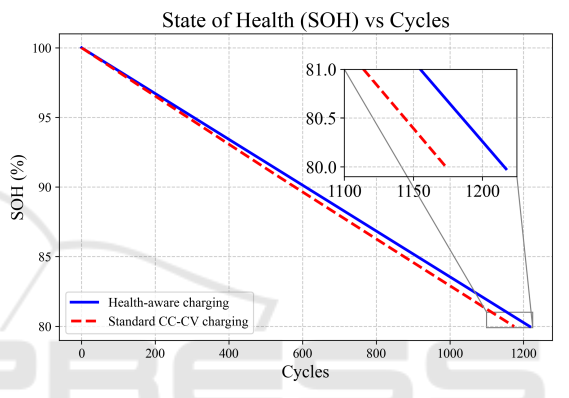


Figure 9: Comparison of Health-Aware and Standard CC-CV Charging Methods with UDDS discharge cycles with control model in loop.

a longer sequence of typical discharge cycles.

Remark 4. In the Health-aware optimization formulation, the SOH_0 is not fixed to the initial cycle value. Instead, it is updated dynamically at the beginning of each new charge cycle or just before the new MPC horizon. This allows the charging current to adapt to the current health state of the battery, keeping the charging profile efficient.

On applying our health aware charging strategy at 3C rate, the battery's degradation is reduced, as is illustrated in figure 9. It achieves this by dynamically utilizing the current states and optimizing the charging profile, while still minimizing the SOH degradation during charging. In contrast, the standard CC-CV charging method follows a fixed rule-based approach, applying a constant current followed by a constant voltage, without taking the battery's health into account. This can lead to faster degradation. As compared to the standard CC-CV charging, the health-aware optimal charging lasts for approximately 2.5% more cycles.

Finally, we study how the proposed health-aware controller would react in realistic conditions, in closed

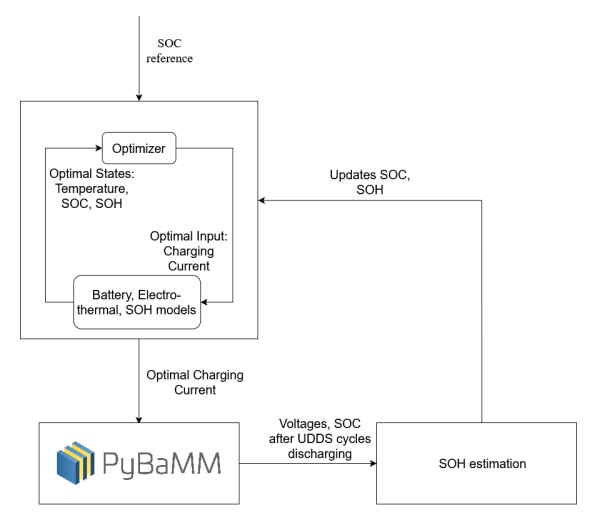


Figure 10: Configuration with PyBaMM emulation in the loop.

loop, with imperfect models. To do so, we have set up the configuration as shown in Figure 10, with the controller actions being applied to the high-fidelity PyBaMM model, and receiving updates from it, to which the controller then reacts.

Remark 5. In the closed-loop simulations, the expected degradation prediction is transformed into the change in SOH for the degradation penalizing term.

Initially, the health-aware optimal control gives an optimal charging current profile, for a specified SOC reference and the system's present states, including the temperature, SOC, overpotential, and SOH. It should also be noted that the control is calculated using the models from section 2, which are far simpler than the full PyBaMM model. This profile is then applied to the PyBaMM model. The simulation outcomes, which provide updated SOC and SOH *estimates*, are fed back into our health-aware optimal control optimizer.

Remark 6. It should be noted that the the discharge cycle in these simulations has a lower DoD during the UDDS discharging profile, and so eventually the charging has a less depth of charge. This choice is driven by the need for stable PyBaMM in closed loop simulations.

Figure 11 shows the SOH degradation over a span of 5000 cycles for both the charging strategies i.e., CC-CV charging and Health-aware charging. It can be observed that Health-aware charging retains approximately 90% of its SOH, while CC-CV falls to approximately 88.7%. It is also evident that Health-aware charging had approximately 600 more cycles than CC-CV method before reaching 90% SOH. This disparity occurs because the CC-CV charging strategy is purely voltage and C-rate without regard to the state of health or degradation impacts. While, the health-

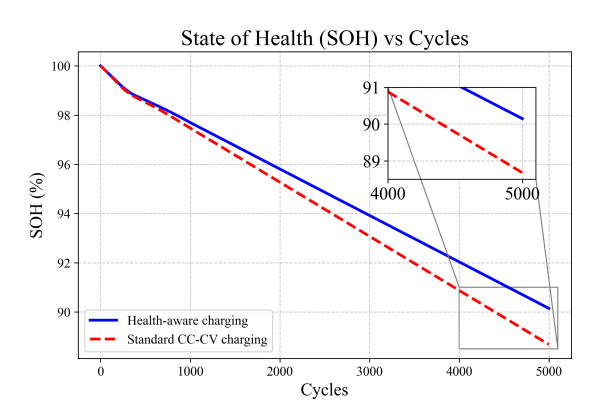


Figure 11: Comparison of Health-Aware and Standard CC-CV Charging Methods with UDDS discharge cycles with PyBaMM in closed-loop.

aware charging explicitly considers battery's updated SOH during optimization. Due to this, the charging current prevents excessive degradation and prolongs battery. Eventually, the figure highlights the impact of considering SOH in Health-aware charging leading to better performance than standard CC-CV.

5 CONCLUSION

This paper presents a health-aware MPC based battery charging approach integrating electrical, thermal and degradation dynamics via Bayesian Networks. We validated our approach through high-fidelity simulations and it demonstrated reduced SOH degradation compared to standard CC-CV methods. The difference represents a significant enhancement in life-cycle sustainability especially for long-term applications.

We expect SOH estimation and corresponding charging profiles to become increasingly important, due to (i) the increasing utilization of e.g., EVs, but (ii) as battery passports gradually become standardized, to keep track of battery health, since then there will be extra incentives to ensure batteries are not degraded by inefficient charging.

While the proposed approach demonstrates promising results in high-fidelity simulations, real-world experimental validation is essential to assess its robustness, practical feasibility and generalization. Future work will focus on implementing the methodology on actual battery systems, with significant emphasis on developing and validating robust estimators. Furthermore, the current deterministic control formulation does not utilize the uncertainty propagation from the BN degradation model. Future work will address these gaps by integrating stochastic MPC strategies.

ACKNOWLEDGMENT

This research was supported by Flanders Make, the strategic research centre for the manufacturing industry in Belgium, in the framework of the OptiBATT_IRVA project.

REFERENCES

- Abdollahi, A., Han, X., Avvari, G., Raghunathan, N., Balasingam, B., Pattipati, K. R., and Bar-Shalom, Y. (2016). Optimal battery charging, part i: Minimizing time-to-charge, energy loss, and temperature rise for ocv-resistance battery model. *Journal of Power Sources*, 303:388–398.
- Agency, I. E. (2024). Global ev outlook 2024: Moving towards increased affordability.
- Akbarzadeh, M., Kalogiannis, T., Jaguemont, J., He, J., Jin, L., Berecibar, M., and Van Mierlo, J. (2020). Thermal modeling of a high-energy prismatic lithium-ion battery cell and module based on a new thermal characterization methodology. *Journal of Energy Storage*, 32:101707.
- Andersson, J. A., Gillis, J., Horn, G., Rawlings, J. B., and Diehl, M. (2019). Casadi: a software framework for nonlinear optimization and optimal control. *Mathematical Programming Computation*, 11:1–36.
- Bazlen, S., Heugel, P., von Kessel, O., Commerell, W., and Tübke, J. (2022). Influence of charging protocols on the charging capability and aging of lithium-ion cells with silicon-containing anodes. *Journal of Energy Storage*, 49:104044.
- Birkl, C. R., Roberts, M. R., McTurk, E., Bruce, P. G., and Howey, D. A. (2017). Degradation diagnostics for lithium ion cells. *Journal of Power Sources*, 341:373– 386.
- Cai, Y., Che, Y., Li, H., Jiang, M., and Qin, P. (2021). Electro-thermal model for lithium-ion battery simulations. *Journal of Power Electronics*, 21(10):1530–1541.
- Christophersen, J. P. (2015). Battery test manual for electric vehicles, revision 3. Technical report, Idaho National Lab.(INL), Idaho Falls, ID (United States).
- den Boef, P., Cox, P. B., and Tóth, R. (2021). Lpvcore: Matlab toolbox for lpv modelling, identification and control. *IFAC-PapersOnLine*, 54(7):385–390.
- Erdinc, O., Vural, B., and Uzunoglu, M. (2009). A dynamic lithium-ion battery model considering the effects of temperature and capacity fading. In 2009 International Conference on Clean Electrical Power, pages 383–386. IEEE
- Gillis, J., Vandewal, B., Pipeleers, G., and Swevers, J. (2020). Effortless modeling of optimal control problems with rockit. In 39th Benelux Meeting on Systems and Control, volume 138. Elspeet, The Netherlands.
- Hoekstra, F., Donkers, M., and Bergveld, H. (2023). Rapid empirical battery electromotive-force and overpotential

- modelling using input—output linear parameter-varying methods. *Journal of Energy Storage*, 65:107185.
- Hostens, E., Eryilmaz, K., Vangilbergen, M., and Ooijevaar, T. (2024). Bayesian networks for remaining useful life prediction. In *PHM Society European Conference*, volume 8, pages 11–11.
- Klein, R., Chaturvedi, N. A., Christensen, J., Ahmed, J., Findeisen, R., and Kojic, A. (2011). Optimal charging strategies in lithium-ion battery. In *Proceedings of the 2011 american Control Conference*, pages 382–387. IEEE.
- Li, Y., Li, K., Xie, Y., Liu, J., Fu, C., and Liu, B. (2020). Optimized charging of lithium-ion battery for electric vehicles: Adaptive multistage constant current–constant voltage charging strategy. *Renewable energy*, 146:2688–2699.
- Lu, Y., Han, X., Li, Y., Li, X., and Ouyang, M. (2024). Health-aware fast charging for lithium-ion batteries: Model predictive control, lithium plating detection, and lifelong parameter updates. *IEEE Transactions on Industry Applications*.
- O'Kane, S. E., Ai, W., Madabattula, G., Alonso-Alvarez, D., Timms, R., Sulzer, V., Edge, J. S., Wu, B., Offer, G. J., and Marinescu, M. (2022). Lithium-ion battery degradation: how to model it. *Physical Chemistry Chemical Physics*, 24(13):7909–7922.
- O'Kane, S. E., Campbell, I. D., Marzook, M. W., Offer, G. J., and Marinescu, M. (2020). Physical origin of the differential voltage minimum associated with lithium plating in li-ion batteries. *Journal of The Electrochemical Society*, 167(9):090540.
- Plett, G. L. (2004). Extended kalman filtering for battery management systems of lipb-based hev battery packs:
 Part 3. state and parameter estimation. *Journal of Power sources*, 134(2):277–292.
- Qin, Y., Zuo, P., Chen, X., Yuan, W., Huang, R., Yang, X., Du, J., Lu, L., Han, X., and Ouyang, M. (2022). An ultra-fast charging strategy for lithium-ion battery at low temperature without lithium plating. *Journal of Energy Chemistry*, 72:442–452.
- Sulzer, V., Marquis, S. G., Timms, R., Robinson, M., and Chapman, S. J. (2021). Python battery mathematical modelling (pybamm). *Journal of Open Research Software*, 9(1).
- Tomaszewska, A., Chu, Z., Feng, X., O'kane, S., Liu, X., Chen, J., Ji, C., Endler, E., Li, R., Liu, L., et al. (2019). Lithium-ion battery fast charging: A review. *ETransportation*, 1:100011.
- Van Den Bossche, P. (2010). Iec 61851-1: Electric vehicle conductive charging system-part 1: General requirements. In 2, pages 1–99. Iec.
- Wächter, A. and Biegler, L. T. (2006). On the implementation of an interior-point filter line-search algorithm for large-scale nonlinear programming. *Mathematical programming*, 106:25–57.
- Wassiliadis, N., Kriegler, J., Gamra, K. A., and Lienkamp, M. (2023). Model-based health-aware fast charging to mitigate the risk of lithium plating and prolong the cycle life of lithium-ion batteries in electric vehicles. *Journal of Power Sources*, 561:232586.

Xavier, M. A., de Souza, A. K., and Trimboli, M. S. (2020). A split-future mpc algorithm for lithium-ion battery cell-level fast-charge control. *IFAC-PapersOnLine*, 53(2):12459–12464.

Xavier, M. A. and Trimboli, M. S. (2015). Lithium-ion battery cell-level control using constrained model predictive control and equivalent circuit models. *Journal of Power Sources*, 285:374–384.

